

On the Analysis of Second Order Time Filtered Backward Euler Method for the EMAC Formulation of Navier-Stokes Equations

Medine Demir ^{*} Aytekin Çibik [†] Songül Kaya [‡]

Abstract. This paper considers the backward Euler based linear time filtering method for the EMAC formulation of the incompressible Navier-Stokes equations. The time filtering is added as a modular step to the standard backward Euler code leading to a 2-step, unconditionally stable, second order linear method. Despite its success in conserving important physical quantities when the divergence constraint is only weakly enforced, the EMAC formulation is unable to improve solutions of backward Euler discretized NSE. The combination of the time filtering with the backward Euler discretized EMAC formulation of NSE greatly increases numerical accuracy of solutions and still conserves energy, momentum and angular momentum as EMAC does. Several numerical experiments are provided that both verify the theoretical findings and demonstrate superiority of the proposed method over the unfiltered case.

1 Introduction

Incompressible viscous fluid flows are governed by the Navier-Stokes equations (NSE), which are given as follows:

$$\begin{aligned} \mathbf{u}_t - \nu \Delta \mathbf{u} + \mathbf{u} \cdot \nabla \mathbf{u} + \nabla p &= \mathbf{f} & \text{in } \Omega \times (0, T), \\ \nabla \cdot \mathbf{u} &= 0 & \text{in } \Omega \times (0, T], \\ \mathbf{u} &= \mathbf{0} & \text{in } \partial\Omega \times [0, T], \\ \mathbf{u}(\mathbf{x}, 0) &= \mathbf{u}_0(\mathbf{x}) & \text{for } \mathbf{x} \in \Omega. \end{aligned} \tag{1.1}$$

Here \mathbf{u} represents the velocity, p the zero-mean pressure, \mathbf{f} an external force and ν the kinematic viscosity. Due to its widespread use in both science and engineering, the importance of NSE in computational fluid dynamics is indisputable. Since finding analytical solution is extremely hard, especially under small viscosity, there has been extensive studies for centries on Galerkin finite element methods for incompressible flows, see, e.g., [1, 2, 3, 4, 5, 6, 7]. In classical H -conforming methods, the divergence constraint is only weakly enforced which leads to the loss of numerical accuracy as well as many important conservation laws, including energy, momentum, angular momentum, and others. It is well-known that a good way to measure the accuracy of a model is by how much physical balances it retains. For this purpose, practitioners have developed many numerical methods, see e.g. [5, 8, 9, 11]. However, none of them conserve all the balances of physical quantities at the same time. To handle this issue, in the study [12], the authors introduced a new formulation of NSE by reformulating the nonlinear term, named as the EMAC formulation which is the first scheme conserving all of energy, momentum and angular momentum even when the divergence constraint is not strongly enforced. In the light of many studies following the original paper [12], e.g. [13, 14, 15, 16, 17, 18, 19], the EMAC formulation has proven to exhibit superior performance especially over longer time periods [20] compared to traditionally used schemes. All these studies agree in the opinion that the EMAC formulation reduces numerical dissipation and significantly increases numerical accuracy compared to previously studied ones thanks to its ability to conserve all the physical quantities.

^{*}Department of Mathematics, Middle East Technical University, 06800 Ankara, Turkey; dmedine@metu.edu.tr

[†]Department of Mathematics, Gazi University, 06800 Ankara, Turkey; abayram@gazi.edu.tr

[‡]Department of Mathematics, Middle East Technical University, 06800 Ankara, Turkey; smerdan@metu.edu.tr.

It is well-known that backward Euler (BE) time discretization is one of the most commonly used method to approximate the time dependent viscous flow problems [21, 22] due to its unconditional stability, rapid convergence to analytical solution and easy implementation. However, it should not be forgotten that it tends to produce nonphysical oscillations in the solution [23] for higher time steps even if the method is stable. The way to increase numerical accuracy without the need for a more complex method was first proposed in the study [24] for the ODEs. As stated in [23], by adding only one additional line of code to BE scheme, it is possible to reduce numerical dissipation, to increase accuracy from first order to the second order and to obtain an *A*-stable method with a usefull error estimator. In recent years, this idea was extended to the incompressible NSE in [25], to MHD equations in [26] and to the Boussinesq equations in [27]. The common theme in these studies is that applying the linear time filtering method to BE scheme with constant time step achieves a second order, more accurate and *A* stable method. Moreover, combining the second step with the first step yields a second order accurate method akin to backward differentiation (BDF2) formula and performs a consistent and simple stability/convergence analysis.

The purpose of this report is to investigate the effect of this novel idea from [25] on the EMAC formulation of time-dependent, incompressible fluid flows for constant time steps. Herein, based on the success of EMAC formulation in [12] and time filtering on BE for constant time step in [25], we naturally took the step of combining these two ideas in order to see whether time filtering method will improve the accuracy of solutions of NSE with EMAC formulation. The proposed numerical scheme is a two-step time filtered BE method which is efficient, $O(\Delta t^2)$, A stable and easy to implement into any existing legacy code. In the first step, velocity solutions of the EMAC scheme is calculated with the usual BE finite element discretization, we call as BE-EMAC. The second step post proceeds this velocity approximation by using a second order time filtering under constant step size. Newton method was applied for the EMAC nonlinearity. We show the conservation of the physically conserved quantities such as energy, momentum and angular momentum and we refer it as energy, momentum, angular momentum conserving time filtered formulation (EMAC-FILTERED). Additionally, we provide that the method is both stable and optimally accurate.

The presentation of this paper is as follows. Section 2 provides some notations and mathematical preliminaries needed for a smooth analysis to follow. In section 3, EMAC-FILTERED method is described. Conservation properties are studied in section 4. Section 5 is devoted to a complete stability and convergence analysis of the EMAC-FILTERED method. In section 6, several numerical experiments are performed which tests the conservation properties, the accuracy and efficiency of the method and compares it with BE-EMAC solutions. Finally, conclusions and possible future directions are drawn in section 7.

2 Notations and Mathematical Preliminaries

Let Ω in \mathbb{R}^d , ($d = 2, 3$) is a convex polygonal or polyhedral domain with boundary $\partial\Omega$. The inner product and norm of Lebesgue spaces $(L^p(\Omega))^d$, $1 \leq p \leq \infty$, $p \neq 2$ will be denoted by (\cdot, \cdot) and $\|\cdot\|_{L^p}$, respectively and the norm in Sobolev spaces $(H^k(\Omega))^d$ by $\|\cdot\|_k$ while all other norms will be labelled appropriately. The natural velocity field and pressure spaces will be considered

$$\mathbf{X} := (H_0^1(\Omega))^d := \{v \in L^2(\Omega)^d : \nabla v \in L^2(\Omega)^{d \times d} \text{ and } v = 0 \text{ on } \partial\Omega\}, \quad (2.1)$$

$$Q := L_0^2(\Omega) := \{q \in L^2(\Omega) : \int_{\Omega} q dx = 0\} \quad (2.2)$$

The dual space of $H_0^1(\Omega)$ is denoted by H^{-1} with norm

$$\|\mathbf{f}\|_{-1} = \sup_{0 \neq \mathbf{v} \in \mathbf{V}} \frac{|\langle \mathbf{f}, \mathbf{v} \rangle|}{\|\nabla \mathbf{v}\|}$$

The divergence free subspace \mathbf{V} of \mathbf{X} is defined by:

$$\mathbf{V} := \{\mathbf{v} \in \mathbf{X} : (\nabla \cdot \mathbf{v}, q) = 0, \quad \forall q \in Q\}.$$

The following norms are defined for all Lebesgue measurable $w : [0, T] \rightarrow \mathbf{X}$:

$$\begin{aligned}\|w\|_{L^p(0,T;\mathbf{X})} &= \left(\int_0^T \|w(t)\|_{\mathbf{X}}^p dt \right)^{1/p}, \quad 1 \leq p < \infty \\ \|w\|_{L^\infty(0,T;\mathbf{X})} &= \text{ess sup}_{0 \leq t \leq T} \|w(t)\|_{\mathbf{X}}\end{aligned}$$

For a spatial discretization, let $\mathbf{X}_h \subset \mathbf{X}$, $Q_h \subset Q$ be velocity-pressure finite element spaces defined on a regular, conforming triangulation π_h of the domain Ω with maximum diameter h satisfying the discrete inf-sup condition,

$$\inf_{q_h \in Q_h} \sup_{\mathbf{v}_h \in \mathbf{X}_h} \frac{(q_h, \nabla \cdot \mathbf{v}_h)}{\|\nabla \mathbf{v}_h\| \|q_h\|} \geq \beta > 0. \quad (2.3)$$

where β , a constant independent of the mesh size h . Some examples of such spaces can be seen in [31, 32]. For the stability of the pressure, we assume that \mathbf{X}_h and Q_h satisfy the usual discrete inf-sup condition (2.3). Let define the discreteley divergence-free subspace of \mathbf{X}_h by

$$\mathbf{V}_h := \{\mathbf{v}_h \in \mathbf{X}_h \mid (\nabla \cdot \mathbf{v}_h, q_h) = 0 \ \forall q_h \in Q_h\}$$

The Poincaré-Friedrichs inequality will be used frequently throughout the analysis: there exists a constant $C_{PF} = C_{PF}(\Omega)$, depending only the size of the domain, such that

$$\|\mathbf{u}\| \leq C_{PF} \|\nabla \mathbf{u}\| \quad \forall \mathbf{u} \in H_0^1(\Omega)$$

Also, we need the standard inverse inequality: for any $v \in \mathbf{X}_h$,

$$\|\nabla \mathbf{v}\| \leq Ch^{-1} \|\mathbf{v}\| \quad \forall \mathbf{v} \in H_0^1(\Omega)$$

It is important to note that in most common finite element discretizations of the NSE and related systems, the divergence constraint $\nabla \cdot u_h = 0$ is only weakly enforced which plays a major role in not conserving physical quantities. such as energy, momentum and angular momentum. Under the inf-sup condition 2.3, the variational formulation of NSE (1.1) in (\mathbf{X}_h, Q_h) is equivalent to in (\mathbf{V}_h, Q_h) , see, e.g., [31]. Additionally, the following well-known approximation properties typical of piecewise polynomials of degree $(k, k-1)$ hold for (\mathbf{X}_h, Q_h) , (see, e.g., [28, 29])

$$\inf_{\mathbf{v}_h \in \mathbf{X}_h} (\|(\mathbf{u} - \mathbf{v}_h)\| + h \|\nabla(\mathbf{u} - \mathbf{v}_h)\|) \leq Ch^{k+1} \|\mathbf{u}\|_{k+1} \quad \mathbf{u} \in H^{k+1}(\Omega), \quad (2.4)$$

$$\inf_{q_h \in Q_h} \|p - q_h\| \leq Ch^k \|p\|_k \quad p \in H^k(\Omega). \quad (2.5)$$

For the convergence analysis, we also need the following discrete Gronwall lemma stated in [31] :

Lemma 2.1. (Discrete Gronwall Lemma) Let Δt , M and $\alpha_n, \beta_n, \xi_n, \delta_n$ (for integers $n \geq 0$) be non negative finite numbers such that

$$\alpha_m + \Delta t \sum_{n=0}^m \beta_n \leq \Delta t \sum_{n=0}^m \delta_n \alpha_n + \Delta t \sum_{n=0}^m \xi_n + M \quad (2.6)$$

Suppose that $\Delta t \delta_n < 1$ for all n . Then,

$$\alpha_m + \Delta t \sum_{n=0}^m \beta_n \leq \exp \left(\Delta t \sum_{n=0}^m \beta_n \frac{\delta_n}{1 - \Delta t \delta_n} \right) \left(\Delta t \sum_{n=0}^m \xi_n + M \right) \quad \text{for } m \geq 0 \quad (2.7)$$

2.1 Vector identities and trilinear forms

For a sufficiently smooth velocity field \mathbf{u} , let denote the symmetric part of $\nabla \mathbf{u}$ by $\mathbf{D}(\mathbf{u}) = \frac{\nabla \mathbf{u} + (\nabla \mathbf{u})^T}{2}$ which is the rate of deformation tensor. The following identity is the key idea for the EMAC formulation

$$(\mathbf{u} \cdot \nabla) \mathbf{u} = 2\mathbf{D}(\mathbf{u})\mathbf{u} - \frac{1}{2} \nabla |\mathbf{u}|^2,$$

for which the inertia term is splitted into the acceleration driven by $2\mathbf{D}(\mathbf{u})$ and potential term further absorbed by redefined pressure. Following [33], the trilinear form for EMAC formulation is defined by

$$c(\mathbf{u}, \mathbf{v}, \mathbf{w}) = 2(\mathbf{D}(\mathbf{u})\mathbf{v}, \mathbf{w}) + ((\nabla \cdot \mathbf{u})\mathbf{v}, \mathbf{w})$$

Herein and the rest of this section, we assume $\mathbf{u}, \mathbf{v}, \mathbf{w} \in \mathbf{X}$, i.e. no divergence free condition is assumed for any of $\mathbf{u}, \mathbf{v}, \mathbf{w}$. It is critical to add the divergence term in the definition of $c(\cdot, \cdot, \cdot)$ to satisfy the cancellation property:

$$c(\mathbf{v}, \mathbf{v}, \mathbf{v}) = 0$$

We use the following identities

$$(\mathbf{u} \cdot \nabla \mathbf{v}, \mathbf{w}) = -(\mathbf{u} \cdot \nabla \mathbf{w}, \mathbf{v}) - ((\nabla \cdot \mathbf{u})\mathbf{v}, \mathbf{w}), \quad (2.8)$$

$$(\mathbf{u} \cdot \nabla \mathbf{w}, \mathbf{w}) = -\frac{1}{2}((\nabla \cdot \mathbf{u})\mathbf{w}, \mathbf{w}), \quad (2.9)$$

$$(\mathbf{u} \cdot \nabla \mathbf{v}, \mathbf{w}) = ((\nabla \mathbf{v})\mathbf{u}, \mathbf{w}) = ((\nabla \mathbf{v})^T \mathbf{w}, \mathbf{u}). \quad (2.10)$$

3 The EMAC-FILTERED scheme

We consider the following weak formulation of the EMAC formulation of 1.1: Find $\mathbf{u} : (0, T] \rightarrow \mathbf{X}$, $p : (0, T] \rightarrow Q$ satisfying

$$(\mathbf{u}_t, \mathbf{v}) + \nu(\nabla \mathbf{u}, \nabla \mathbf{v}) + c(\mathbf{u}, \mathbf{u}, \mathbf{v}) - (P, \nabla \cdot \mathbf{v}) = (\mathbf{f}, \mathbf{v}) \quad \forall \mathbf{v} \in \mathbf{X} \quad (3.1)$$

$$(q, \nabla \cdot \mathbf{u}) = 0 \quad \forall q \in Q, \quad (3.2)$$

where P is defined as $P = p - \frac{1}{2}|\mathbf{u}|^2$ and $\mathbf{u}(0, \mathbf{x}) = \mathbf{u}_0(\mathbf{x}) \in \mathbf{X}$. Here, we use the EMAC form of the nonlinear term. We now present the two step time filtered numerical scheme of (3.1)-(3.2) for constant time step. In the first step, the velocity approximation of the scheme (3.1)-(3.2) is calculated with the usual BE finite element (fully implicit) discretization and the second step introduces a simple time filter which combines this velocity solution linearly with the solutions at previously time levels. The second step greatly increases time accuracy although it does not significantly alter system complexity. The modular time filtered numerical scheme of (3.1)-(3.2) of the NSE with EMAC formulation reads as follows:

Algorithm 3.1. Let body force \mathbf{f} and the initial condition \mathbf{u}_0 be given. Select T as the end time, and let N be the number of time steps to take the time step size $\Delta t = T/N$. Define $\mathbf{u}_h^0, \mathbf{u}_h^{-1}$ as the nodal interpolants of \mathbf{u}_0 , then for any $n \geq 1$ ($n = 0, 1, \dots, N-1$), find $(\mathbf{u}_h^{n+1}, P_h^{n+1}) \in (\mathbf{X}_h, Q_h)$ via the following two steps:

Step 1: Compute $(\tilde{\mathbf{u}}_h^{n+1}, P_h^{n+1}) \in (\mathbf{X}_h, Q_h)$ such that

$$\left(\frac{\tilde{\mathbf{u}}_h^{n+1} - \mathbf{u}_h^n}{\Delta t}, \mathbf{v}_h \right) + \nu(\nabla \tilde{\mathbf{u}}_h^{n+1}, \nabla \mathbf{v}_h) + c(\tilde{\mathbf{u}}_h^{n+1}, \tilde{\mathbf{u}}_h^{n+1}, \mathbf{v}_h) - (P_h^{n+1}, \nabla \cdot \mathbf{v}_h) = (\mathbf{f}(t^{n+1}), \mathbf{v}_h), \quad (3.3)$$

$$(\nabla \cdot \tilde{\mathbf{u}}_h^{n+1}, q_h) = 0. \quad (3.4)$$

Step 2:

$$\mathbf{u}_h^{n+1} = \tilde{\mathbf{u}}_h^{n+1} - \frac{1}{3}(\tilde{\mathbf{u}}_h^{n+1} - 2\mathbf{u}_h^n + \mathbf{u}_h^{n-1}) \quad (3.5)$$

for all $(\mathbf{v}_h, q_h) \in (\mathbf{X}_h, Q_h)$.

We note that, Step 1 is the standard backward Euler scheme for the NSE. Step 2 is just a post processing step to apply easily implemented linear time filter which clearly makes the method numerically efficient.

Define the interpolation operator F as

$$F[\mathbf{w}_h^{n+1}] = \frac{3}{2}\mathbf{w}_h^{n+1} - \mathbf{w}_h^n + \frac{1}{2}\mathbf{w}_h^{n-1} \quad (3.6)$$

which is formally $F[\mathbf{w}_h^{n+1}] = \mathbf{w}_h^{n+1} + O(\Delta t^2)$. Rewriting (3.5) as $\tilde{\mathbf{u}}_h^{n+1} = \frac{3}{2}\mathbf{u}_h^{n+1} - \mathbf{u}_h^n + \frac{1}{2}\mathbf{u}_h^{n-1}$ and inserting in (3.3)-(3.4) along with (3.6), the following equivalent method is obtained.

$$\frac{1}{\Delta t} \left(\frac{3}{2}\mathbf{u}_h^{n+1} - 2\mathbf{u}_h^n + \frac{1}{2}\mathbf{u}_h^{n-1}, \mathbf{v}_h \right) + \nu(\nabla(F[\mathbf{u}_h^{n+1}]), \nabla \mathbf{v}_h) + c(F[\mathbf{u}_h^{n+1}], F[\mathbf{u}_h^{n+1}], \mathbf{v}_h) \quad (3.7)$$

$$- (P_h^{n+1}, \nabla \cdot \mathbf{v}_h) = (f(t^{n+1}), \mathbf{v}_h) \quad (3.7)$$

$$(\nabla \cdot (F[\mathbf{u}_h^{n+1}]), q_h) = 0 \quad (3.8)$$

for all $(\mathbf{v}_h, q_h) \in (\mathbf{X}_h, Q_h)$. For a simple analysis, the equivalent formulation (3.7)-(3.8) of the method will be used for the complete stability and convergence analysis while (3.3)-(3.5) will be considered in the implementation of the method for computer simulations.

Remark: We emphasize here that although the time derivative is discretized by using classical BDF2 time stepping method, the other terms are not. Thus, the method should not be considered as the standard BDF2 method.

The analysis of the method requires the definition of G -norm and F -norm. Since G -stability refers to A -stability, the G -matrix is often used in BDF2 analysis, see e.g., [34] and references therein. With respect to the definition of G -matrix in [35], with the choices of $\theta = 1$ and $\nu = 2\epsilon$, the G -matrix of the described method is follows,

$$G = \begin{pmatrix} \frac{3}{2} & -\frac{3}{4} \\ -\frac{3}{4} & \frac{1}{2} \end{pmatrix}$$

with the G -norm

$$\left\| \begin{bmatrix} \mathbf{u} \\ \mathbf{v} \end{bmatrix} \right\|_G^2 = \left(\begin{bmatrix} \mathbf{u} \\ \mathbf{v} \end{bmatrix}, G \begin{bmatrix} \mathbf{u} \\ \mathbf{v} \end{bmatrix} \right) \quad (3.9)$$

which can be negative. Here $\begin{bmatrix} \mathbf{u} \\ \mathbf{v} \end{bmatrix}$ is $2n$ vector.

Additionally, we use a symmetric positive matrix $F = 3I \in \mathbb{R}^{n \times n}$ which is defined in details in [35]. For any $\mathbf{u} \in \mathbb{R}^n$, define F norm of the n vector \mathbf{u} by

$$\|\mathbf{u}\|_F = (\mathbf{u}, F\mathbf{u}) \quad (3.10)$$

The following properties of G -norm are well known and see, [34, 35] for a detailed derivation of these estimations.

Lemma 3.1. *L^2 norm and G -norm are equivalent in the following sense: there exists constants $C_1 > C_2 > 0$ such that*

$$C_1 \left\| \begin{bmatrix} \mathbf{u} \\ \mathbf{v} \end{bmatrix} \right\|_G^2 \leq \left\| \begin{bmatrix} \mathbf{u} \\ \mathbf{v} \end{bmatrix} \right\|^2 \leq C_2 \left\| \begin{bmatrix} \mathbf{u} \\ \mathbf{v} \end{bmatrix} \right\|_G^2$$

Lemma 3.2. *The symmetric positive matrix $F \in \mathbb{R}^{n \times n}$ and the symmetric matrix $G \in \mathbb{R}^{2n \times 2n}$ satisfy the following equality:*

$$\begin{aligned} & \left(\frac{\frac{3}{2}w_{n+1} - 2w_n + \frac{1}{2}w_{n-1}}{\Delta t}, \frac{3}{2}w_{n+1} - w_n + \frac{1}{2}w_{n-1} \right) \\ &= \frac{1}{\Delta t} \left\| \begin{bmatrix} w_{n+1} \\ w_n \end{bmatrix} \right\|_G^2 - \frac{1}{\Delta t} \left\| \begin{bmatrix} w_n \\ w_{n-1} \end{bmatrix} \right\|_G^2 + \frac{1}{4\Delta t} \|w_{n+1} - 2w_n + w_{n-1}\|_F^2 \end{aligned} \quad (3.11)$$

Lemma 3.3. For any $\mathbf{u}, \mathbf{v} \in R^n$, we have

$$(\begin{bmatrix} \mathbf{u} \\ \mathbf{v} \end{bmatrix}, G \begin{bmatrix} \mathbf{u} \\ \mathbf{v} \end{bmatrix}) \geq \frac{3}{4} \|\mathbf{u}\|^2 - \frac{1}{4} \|\mathbf{v}\|^2, \quad (3.12)$$

$$(\begin{bmatrix} \mathbf{u} \\ \mathbf{v} \end{bmatrix}, G \begin{bmatrix} \mathbf{u} \\ \mathbf{v} \end{bmatrix}) \leq \frac{3}{2} \|\mathbf{u}\|^2 + \frac{3}{4} \|\mathbf{v}\|^2. \quad (3.13)$$

Proof. Taking $\theta = 1$ and $\nu = 2\epsilon$ in Lemma 3.1 of [35] gives the result. \square

In the analysis, we need also the following consistency error estimations.

Lemma 3.4. There exists $C > 0$ such that

$$\Delta t \sum_{n=1}^{N-1} \left\| F[\mathbf{w}^{n+1}] - \mathbf{w}^{n+1} \right\|^2 \leq C \Delta t^4 \|\mathbf{w}_{tt}\|_{L^2(0,T;L^2(\Omega))} \quad (3.14)$$

$$\Delta t \sum_{n=1}^{N-1} \left\| \frac{3w_{n+1} - 4w_n + w_{n-1}}{2\Delta t} - \mathbf{w}^{n+1} \right\|^2 \leq C \Delta t^4 \|\mathbf{w}_{ttt}\|_{L^2(0,T;L^2(\Omega))} \quad (3.15)$$

Proof. The reader is referred to [26] for a detailed proof. \square

4 Conservation Laws

In this section, we investigate the conservation of the integral variants of fluid flow energy, momentum and angular momentum for Algorithm 3.1. It is well known that the physical accuracy of a model is measured by how well its solutions preserve these quantities. For NSE, energy, momentum and angular momentum are defined by

$$\text{Kinetic Energy } E = \frac{1}{2}(\mathbf{u}, \mathbf{u}) = \frac{1}{2} \int_{\Omega} |\mathbf{u}|^2 d\vec{x},$$

$$\text{Linear Momentum } M = \int_{\Omega} \mathbf{u} d\vec{x},$$

$$\text{Angular Momentum } M_x = \int_{\Omega} \mathbf{u} \times \vec{x} d\vec{x}.$$

Let e_i be the i -th unit vector and $\phi_i = x \times e_i$. Then, momentum and angular momentum can be equivalently defined as:

$$M_i = \int_{\Omega} \mathbf{u}_i d\vec{x} = (\mathbf{u}, e_i),$$

$$(M_x)_i = \int_{\Omega} (\mathbf{u} \times x) \cdot e_i d\vec{x} = (\mathbf{u}, \phi_i).$$

To obtain the balances, assume that the solutions \mathbf{u}, p have compact support in Ω (e.g. consider an isolated vortex). We first state the energy balance of the EMAC-FILTERED scheme (3.7)-(3.8).

Theorem 4.1. EMAC-FILTERED scheme (3.7)-(3.8) satisfies the discrete energy balance for $\nu = 0, f = 0$:

$$\begin{aligned} & \left\| \begin{bmatrix} \mathbf{u}_h^N \\ \mathbf{u}_h^{N-1} \end{bmatrix} \right\|_G^2 + \Delta t \sum_{n=1}^{N-1} (\nu \|\nabla F[\mathbf{u}_h^{n+1}]\|^2) + \frac{1}{4} \sum_{n=1}^{N-1} \|\mathbf{u}_h^{n+1} - 2\mathbf{u}_h^n + \mathbf{u}_h^{n-1}\|_F^2 \\ &= \left\| \begin{bmatrix} \mathbf{u}_h^1 \\ \mathbf{u}_h^0 \end{bmatrix} \right\|_G^2 + \Delta t \sum_{n=1}^{N-1} (\mathbf{f}(t^{n+1}), F[\mathbf{u}_h^{n+1}]) \end{aligned} \quad (4.1)$$

Proof. Set $\mathbf{v}_h = F[\mathbf{u}_h^{n+1}]$ in (3.7), $q_h = p_h^{n+1}$ in (3.8), then the nonlinear term and pressure term vanishes and we get by Lemma 3.2

$$\frac{1}{\Delta t} \left\| \begin{bmatrix} \mathbf{u}_h^{n+1} \\ \mathbf{u}_h^n \end{bmatrix} \right\|_G^2 - \frac{1}{\Delta t} \left\| \begin{bmatrix} \mathbf{u}_h^n \\ \mathbf{u}_h^{n-1} \end{bmatrix} \right\|_G^2 + \frac{1}{4\Delta t} \|\mathbf{u}_h^{n+1} - 2\mathbf{u}_h^n + \mathbf{u}_h^{n-1}\|_F^2 + \nu \|\nabla F[\mathbf{u}_h^{n+1}]\|^2 = (\mathbf{f}(t^{n+1}), F[\mathbf{u}_h^{n+1}]) \quad (4.2)$$

Next, multiplying both sides of (4.2) by Δt and taking sum from $n = 1$ to $N - 1$ proves the result. \square

Next, we consider the conservation of momentum and angular momentum of the algorithm 3.1. Let Ω_s be a strip around $\partial\Omega$ and Ω_i be such that $\Omega = \Omega_s \cup \Omega_i$. Let also define $\chi(g) \in \mathbf{X}$ to the restriction of some arbitrary function g by setting $\chi(g) = g$ in Ω and arbitrarily defined elsewhere to meet the boundary conditions such that $\chi(g) = g$ in Ω_i but $g|_{\partial\Omega} = 0$. Based on [12], we assume that $\mathbf{u}_h = 0$ and $p_h = 0$ on Ω_s .

Theorem 4.2. For $\nu = 0, f = 0$, EMAC-FILTERED scheme (3.7)-(3.8) conserves momentum and angular momentum for all $t > 0$:

$$M_{Emac-Fil}(t) = M_{Emac-Fil}(0)$$

Proof. We start by showing momentum conservation. Choose $\mathbf{v}_h = \chi(e_i)$ in (3.7) to get

$$((\mathbf{u}_h)_t, e_i) + \nu(\nabla F[\mathbf{u}_h^{n+1}], \nabla e_i) + c(F[\mathbf{u}_h^{n+1}], F[\mathbf{u}_h^{n+1}], e_i) = (\mathbf{f}(t^{n+1}), e_i) \quad (4.3)$$

For the nonlinear term, expanding the rate of deformation tensor and using the identity (2.8) with the fact that e_i is divergence-free yields

$$\begin{aligned} c(F[\mathbf{u}_h^{n+1}], F[\mathbf{u}_h^{n+1}], e_i) &= 2(\mathbf{D}(F[\mathbf{u}_h^{n+1}])F[\mathbf{u}_h^{n+1}], e_i) + (div(F[\mathbf{u}_h^{n+1}])F[\mathbf{u}_h^{n+1}], e_i) \\ &= (F[\mathbf{u}_h^{n+1}] \cdot \nabla F[\mathbf{u}_h^{n+1}], e_i) + (F[\mathbf{u}_h^{n+1}], \nabla F[\mathbf{u}_h^{n+1}], e_i) + ((\nabla \cdot F[\mathbf{u}_h^{n+1}])F[\mathbf{u}_h^{n+1}], e_i) \\ &= (e_i, \nabla F[\mathbf{u}_h^{n+1}], F[\mathbf{u}_h^{n+1}]) \\ &= 0 \end{aligned}$$

Under the assumption $\nu = 0, f = 0$, one get

$$\frac{d}{dt}(\mathbf{u}_h, e_i) = 0$$

which is precisely the conservation of momentum.

For conservation of angular momentum, take $\mathbf{v}_h = \chi(\phi_i)$ in (3.1) to get

$$((\mathbf{u}_h)_t, \phi_i) + \nu(\nabla F[\mathbf{u}_h^{n+1}], \nabla \phi_i) + c(F[\mathbf{u}_h^{n+1}], F[\mathbf{u}_h^{n+1}], \phi_i) = (\mathbf{f}(t^{n+1}), \phi_i)$$

In a similar manner, by using the identities (2.8) and (2.9) respectively along with $\nabla \cdot \phi_i = 0$, the nonlinear term reduces to

$$\begin{aligned} c(F[\mathbf{u}_h^{n+1}], F[\mathbf{u}_h^{n+1}], \phi_i) &= 2(\mathbf{D}(F[\mathbf{u}_h^{n+1}])F[\mathbf{u}_h^{n+1}], \phi_i) + (div(F[\mathbf{u}_h^{n+1}])F[\mathbf{u}_h^{n+1}], \phi_i) \\ &= (F[\mathbf{u}_h^{n+1}] \cdot \nabla F[\mathbf{u}_h^{n+1}], \phi_i) + (F[\mathbf{u}_h^{n+1}], \nabla F[\mathbf{u}_h^{n+1}], \phi_i) + ((\nabla \cdot F[\mathbf{u}_h^{n+1}])F[\mathbf{u}_h^{n+1}], \phi_i) \\ &= (F[\mathbf{u}_h^{n+1}] \cdot \nabla F[\mathbf{u}_h^{n+1}], \phi_i) + ((\nabla F[\mathbf{u}_h^{n+1}])F[\mathbf{u}_h^{n+1}], \phi_i) \\ &= -(F[\mathbf{u}_h^{n+1}] \cdot \nabla \phi_i, F[\mathbf{u}_h^{n+1}]) \end{aligned}$$

Expanding out the last term gives $(F[\mathbf{u}_h^{n+1}] \cdot \nabla \phi_i, F[\mathbf{u}_h^{n+1}]) = 0$ which vanishes the nonlinear term. Thus, if $\nu = 0, f = 0$ one get

$$\frac{d}{dt}(\mathbf{u}_h, \phi_i) = 0$$

which is angular momentum conservation. \square

5 Numerical Analysis

This section provides unconditional stability result and convergence analysis of the proposed Algorithm 3.1. We first provide the stability analysis of the method.

Lemma 5.1. *Let $\mathbf{f} \in L^\infty(0, T; H^{-1}(\Omega))$. Then for all $\Delta t > 0$ and $N \geq 1$, the solution of the algorithm 3.1 is unconditionally stable in the following sense:*

$$\begin{aligned} \|\mathbf{u}_h^N\|^2 &+ \frac{1}{3} \sum_{n=1}^{N-1} \|\mathbf{u}_h^{n+1} - 2\mathbf{u}_h^n + \mathbf{u}_h^{n-1}\|_F^2 + \frac{2\Delta t \nu}{3} \sum_{n=1}^{N-1} \|\nabla F[\mathbf{u}_h^{n+1}]\|^2 \\ &\leq \left(\frac{1}{3}\right)^N \|\mathbf{u}_h^0\|^2 + 2N(\|\mathbf{u}_h^1\|^2 + \|\mathbf{u}_h^0\|^2) + \frac{2N\Delta t \nu^{-1}}{3} \sum_{n=1}^{N-1} \|\mathbf{f}(t^{n+1})\|^2 \end{aligned} \quad (5.1)$$

Proof. We start the proof by the global energy conservation (4.1).

$$\begin{aligned} \left\| \begin{bmatrix} \mathbf{u}_h^N \\ \mathbf{u}_h^{N-1} \end{bmatrix} \right\|_G^2 &+ \frac{1}{4} \sum_{n=1}^{N-1} \|\mathbf{u}_h^{n+1} - 2\mathbf{u}_h^n + \mathbf{u}_h^{n-1}\|_F^2 + \Delta t \sum_{n=1}^{N-1} (\nu \|\nabla F[\mathbf{u}_h^{n+1}]\|^2) \\ &= \left\| \begin{bmatrix} \mathbf{u}_h^1 \\ \mathbf{u}_h^0 \end{bmatrix} \right\|_G^2 + \Delta t \sum_{n=1}^{N-1} (\mathbf{f}(t^{n+1}), F[\mathbf{u}_h^{n+1}]) \end{aligned} \quad (5.2)$$

The application of Cauchy-Schwarz inequality, Young's inequality and the dual norm on the forcing term gives

$$(\mathbf{f}(t^{n+1}), F[\mathbf{u}_h^{n+1}]) \leq \frac{\nu^{-1} \Delta t}{2} \|\mathbf{f}(t^{n+1})\|_{-1}^2 + \frac{\nu \Delta t}{2} \|\nabla F[\mathbf{u}_h^{n+1}]\|^2, \quad (5.3)$$

Inserting the estimate in (5.2) and applying Lemma 3.3 leads to

$$\begin{aligned} \frac{3}{4} \|\mathbf{u}_h^N\|^2 &+ \frac{1}{4} \sum_{n=1}^{N-1} \|\mathbf{u}_h^{n+1} - 2\mathbf{u}_h^n + \mathbf{u}_h^{n-1}\|_F^2 + \frac{\nu \Delta t}{2} \sum_{n=1}^{N-1} (\|\nabla F[\mathbf{u}_h^{n+1}]\|^2) \\ &\leq \frac{1}{4} \|\mathbf{u}_h^{N-1}\|^2 + \frac{3}{2} \|\mathbf{u}_h^1\|^2 + \frac{3}{4} \|\mathbf{u}_h^0\|^2 + \frac{\nu^{-1} \Delta t}{2} \|\mathbf{f}(t^{n+1})\|_{-1}^2 \end{aligned} \quad (5.4)$$

Lastly, the proof is completed by multiplying by $\frac{4}{3}$ and using the induction. \square

We proceed to present a detailed convergence analysis of the proposed time filtered method for NSE equations with Emac formulation. We use the following notations for the discrete norms. For $\mathbf{v}^n \in H^p(\Omega)$, we define :

$$\|\mathbf{v}\|_{\infty,p} := \max_{0 \leq n \leq N} \|\mathbf{v}^n\|_p, \quad \|\mathbf{v}\|_{m,p} := \left(\Delta t \sum_{n=0}^N \|\mathbf{v}^n\|_p^m \right)^{\frac{1}{m}}.$$

For the optimal asymptotic error estimation, we assume that the following regularity assumptions holds for the exact solution of (1.1):

$$\begin{aligned} \mathbf{u} &\in L^\infty(0, T; H^1(\Omega)) \cap H^1(0, T; H^{k+1}(\Omega)) \cap H^3(0, T; L^2(\Omega)) \cap H^2(0, T; H^1(\Omega)), \\ p &\in L^2(0, T; H^{s+1}(\Omega)), \\ f &\in L^2(0, T; L^2(\Omega)). \end{aligned} \quad (5.5)$$

Theorem 5.1. *Let (\mathbf{u}, p) be the solution of NSE (1.1) such that the regularity assumptions (5.5) are satisfied. Then, under the following time step condition*

$$\Delta t \leq C(\|\nabla F[\mathbf{u}^{n+1}]\|_{\infty,0})^{-1}$$

, the following bound holds for the error $e_{\mathbf{u}}^n = \mathbf{u}^n - \mathbf{u}_h^n$

$$\begin{aligned}
& \|e_{\mathbf{u}}^N\|^2 + \frac{1}{3} \sum_{n=1}^{N-1} \|e_{\mathbf{u}}^{n+1} - 2\mathbf{e}_{\mathbf{u}}^n + \mathbf{e}_{\mathbf{u}}^{n-1}\|_F^2 + \frac{2\Delta t \nu}{3} \sum_{n=1}^{N-1} \|\nabla F[e_{\mathbf{u}}^{n+1}]\|^2 \\
& \leq \left(\frac{1}{3} \right)^N \|\mathbf{e}_{\mathbf{u}}^0\|^2 + 2N(\|\mathbf{e}_{\mathbf{u}}^1\|^2 + \|\mathbf{e}_{\mathbf{u}}^0\|^2) + C \left[\nu^{-1} h^{2k+2} \|\mathbf{u}\|_{2,k+1}^2 + \nu h^{2k} \|\mathbf{u}\|_{2,k+1}^2 + \nu^{-1} h^{2k} \|P^{n+1}\|_{2,k}^2 \right. \\
& \quad \left. + \nu^{-1} \Delta t^4 \|\mathbf{u}_{ttt}\|_{L^2(0,T;L^2(\Omega))}^2 + \Delta t^4 (\nu + \nu^{-1} (\|\nabla F[\mathbf{u}^{n+1}]\|_{\infty,0} + \|\nabla \mathbf{u}^{n+1}\|_{\infty,0})) \|\nabla \mathbf{u}_{tt}\|_{L^2(0,T;L^2(\Omega))}^2 \right. \\
& \quad \left. + \nu^{-1} \left(\|\nabla F[\mathbf{u}^{n+1}]\|_{\infty,0} h^{2k+1} \|\mathbf{u}\|_{2,k+1}^2 + \|\nabla F[\mathbf{u}^{n+1}]\|_{\infty,0} \|F[\mathbf{u}^{n+1}]\|_{\infty,0} h^{2k} \|\mathbf{u}\|_{2,k+1}^2 \right) \right] \quad (5.6)
\end{aligned}$$

where C is a generic constant independent of h and Δt .

Theorem 5.1 with the most common choice of inf-sup stable finite element spaces, like Taylor Hood element, for the velocity and pressure naturally leads to the following Corollary, proving second order accuracy both in time and space.

Corollary 5.1. *Under the assumptions of Theorem 5.1, let $(\mathbf{X}_h, Q_h) = (P_2, P_1)$ be the Taylor-Hood finite element spaces for velocity and pressure. Then, the asymptotic error estimation satisfies, for all $\Delta t > 0$*

$$\begin{aligned}
& \|e_{\mathbf{u}}^N\|^2 + \frac{1}{3} \sum_{n=1}^{N-1} \|e_{\mathbf{u}}^{n+1} - 2\mathbf{e}_{\mathbf{u}}^n + \mathbf{e}_{\mathbf{u}}^{n-1}\|_F^2 + \frac{2\Delta t \nu}{3} \sum_{n=1}^{N-1} \|\nabla F[e_{\mathbf{u}}^{n+1}]\|^2 \\
& \leq C \left(h^4 + \Delta t^4 + \|\mathbf{e}^0\|^2 + \|\mathbf{e}^1\|^2 \right).
\end{aligned}$$

Proof. Application of the approximation properties (2.8)- (2.9) in the right hand side of (5.6) and the regularity assumption (5.5) gives the required result. \square

We now give the proof of our main theorem.

Proof. The proof starts by deriving the error equations. Denote $\mathbf{u}^{n+1} = \mathbf{u}(t^{n+1})$. At time t^{n+1} , the true solution of the NSE (1.1) satisfies

$$\left(\frac{3\mathbf{u}^{n+1} - 4\mathbf{u}^n + \mathbf{u}^{n-1}}{2\Delta t}, \mathbf{v}_h \right) + \nu(\nabla F[\mathbf{u}^{n+1}], \nabla \mathbf{v}_h) + c(F[\mathbf{u}^{n+1}], F[\mathbf{u}^{n+1}], \mathbf{v}_h) - (P^{n+1}, \nabla \cdot \mathbf{v}_h) \quad (5.7)$$

$$= (\mathbf{f}^{n+1}, \mathbf{v}_h) + Intp(\mathbf{u}, \mathbf{v}_h) \quad (5.8)$$

for all $\mathbf{v}_h \in \mathbf{V}_h$ where

$$\begin{aligned}
Intp(\mathbf{u}^{n+1}, \mathbf{v}_h) &= \left(\frac{3\mathbf{u}^{n+1} - 4\mathbf{u}^n + \mathbf{u}^{n-1}}{2\Delta t} - \mathbf{u}_t^{n+1}, \mathbf{v}_h \right) + \nu(\nabla F[\mathbf{u}^{n+1}] - \mathbf{u}^{n+1}, \mathbf{v}_h) \\
&\quad + c(F[\mathbf{u}^{n+1}], F[\mathbf{u}^{n+1}], \mathbf{v}_h) - c(\mathbf{u}^{n+1}, \mathbf{u}^{n+1}, \mathbf{v}_h) \quad (5.9)
\end{aligned}$$

denotes the local truncation error.

Subtracting (3.7) from (5.8) yields

$$\begin{aligned}
& \left(\frac{3e_{\mathbf{u}}^{n+1} - 4e_{\mathbf{u}}^n + e_{\mathbf{u}}^{n-1}}{2\Delta t}, \mathbf{v}_h \right) + \nu(\nabla F[e_{\mathbf{u}}^{n+1}], \nabla \mathbf{v}_h) + c(F[\mathbf{u}^{n+1}], F[\mathbf{u}^{n+1}], \mathbf{v}_h) \\
& \quad - c(F[\mathbf{u}_h^{n+1}], F[\mathbf{u}_h^{n+1}], \mathbf{v}_h) - (P^{n+1}, \nabla \cdot \mathbf{v}_h) = Intp(\mathbf{u}, \mathbf{v}_h) \quad (5.10)
\end{aligned}$$

Decompose the error as

$$e_{\mathbf{u}}^n = \mathbf{u}(t^n) - \mathbf{u}_h^n = (\mathbf{u}(t^n) - I^h \mathbf{u}^n) + (I^h \mathbf{u}^n - \mathbf{u}_h^n) = \eta^n + \phi_h^n. \quad (5.11)$$

where $I^h \mathbf{u}^n$ is an interpolant of \mathbf{u}^n in \mathbf{V}_h . Choosing $\mathbf{v}_h = F[\phi_h^{n+1}]$ in (5.10), using the error decomposition and Lemma 3.2, it follows that

$$\begin{aligned} \frac{1}{\Delta t} \left\| \begin{bmatrix} \phi_h^{n+1} \\ \phi_h^n \end{bmatrix} \right\|_G^2 - \frac{1}{\Delta t} \left\| \begin{bmatrix} \phi_h^n \\ \phi_h^{n-1} \end{bmatrix} \right\|_G^2 &+ \frac{1}{4\Delta t} \|\phi_h^{n+1} - 2\phi_h^n + \phi_h^{n-1}\|_F^2 + \nu \|\nabla F[\phi_h^{n+1}]\|^2 \\ &= \left(\frac{3\eta^{n+1} - 4\eta^n + \eta^{n-1}}{2\Delta t}, F[\phi_h^{n+1}] \right) + \nu(\nabla F[\eta^{n+1}], \nabla F[\phi_h^{n+1}]) \\ &\quad - c(F[\mathbf{u}^{n+1}], F[\mathbf{u}^{n+1}], F[\phi_h^{n+1}]) + c(F[\mathbf{u}_h^{n+1}], F[\mathbf{u}_h^{n+1}], F[\phi_h^{n+1}]) \\ &\quad - (P^{n+1}, \nabla \cdot F[\phi_h^{n+1}]) + \text{Intp}(\mathbf{u}, F[\phi_h^{n+1}]) \end{aligned} \quad (5.12)$$

Next estimate the terms on the RHS of (5.12). The first two terms are bounded by applying Cauchy-Schwarz and Young's inequality:

$$\begin{aligned} \left| - \left(\frac{3\eta^{n+1} - 4\eta^n + \eta^{n-1}}{2\Delta t}, F[\phi_h^{n+1}] \right) \right| &\leq \left\| \frac{3\eta^{n+1} - 4\eta^n + \eta^{n-1}}{2\Delta t} \right\| \|F[\phi_h^{n+1}]\|^2 \\ &\leq \frac{C\nu^{-1}}{\Delta t} \int_{t^{n-1}}^{t^{n+1}} \|\eta_t\|^2 dt + \frac{\nu}{28} \|\nabla F[\phi_h^{n+1}]\|^2 \end{aligned} \quad (5.13)$$

$$\begin{aligned} |\nu(\nabla F[\eta^{n+1}], \nabla F[\phi_h^{n+1}])| &\leq \nu \|\nabla F[\eta^{n+1}]\| \|\nabla F[\phi_h^{n+1}]\| \\ &\leq C\nu \|\nabla F[\eta^{n+1}]\|^2 + \frac{\nu}{28} \|\nabla F[\phi_h^{n+1}]\|^2. \end{aligned} \quad (5.14)$$

Following Theorem 3.2 in [43], the nonlinear terms are estimated as,

$$\begin{aligned} &\left| -c(F[\mathbf{u}^{n+1}], F[\mathbf{u}^{n+1}], F[\phi_h^{n+1}]) + c(F[\mathbf{u}_h^{n+1}], F[\mathbf{u}_h^{n+1}], F[\phi_h^{n+1}]) \right| \\ &\leq C\nu^{-1} \left(\|\nabla F[\mathbf{u}^{n+1}]\|^2 \|F[\eta^{n+1}]\| \|\nabla F[\eta^{n+1}]\| + \|\nabla F[\mathbf{u}^{n+1}]\| \|F[\mathbf{u}^{n+1}]\| \|\nabla F[\eta^{n+1}]\|^2 \right) \\ &\quad + C\nu^{-1} \|\nabla F[\mathbf{u}^{n+1}]\|^2 \|F[\phi_h^{n+1}]\|^2 + \frac{\nu}{28} \|\nabla F[\phi_h^{n+1}]\|^2. \end{aligned} \quad (5.15)$$

For the pressure term, use the fact that $(\nabla \cdot \phi_h, q_h) = 0 \ \forall \phi_h \in \mathbf{V}_h$ together with Cauchy-Schwarz and Young's inequalities to get

$$\begin{aligned} |P^{n+1}, \nabla \cdot \phi_h^{n+1})| &= |(P^{n+1} - q_h, \nabla \cdot \phi_h^{n+1})| \\ &\leq C\nu^{-1} \inf_{q_h \in Q_h} \|P^{n+1} - q_h\|^2 + \frac{\nu}{28} \|\nabla F[\phi_h^{n+1}]\|^2 \end{aligned} \quad (5.16)$$

Next, we proceed to bound the terms in the local truncation error $\text{Intp}(\mathbf{u}, F[\phi_h^{n+1}])$. For the first two terms of $\text{Intp}(\mathbf{u}, F[\phi_h^{n+1}])$, apply the Cauchy-Schwarz Inequality, and Young's inequalities together with the integral remainder form of Taylors theorem to obtain

$$\begin{aligned} &\left| \left(\frac{3\mathbf{u}^{n+1} - 4\mathbf{u}^n + \mathbf{u}^{n-1}}{2\Delta t} - \mathbf{u}_t^{n+1}, F[\phi_h^{n+1}] \right) \right| \\ &\leq \left\| \frac{3\mathbf{u}^{n+1} - 4\mathbf{u}^n + \mathbf{u}^{n-1}}{2\Delta t} - \mathbf{u}_t(t^{n+1}) \right\| \|F[\phi_h^{n+1}]\| \\ &\leq C\Delta t^3 \nu^{-1} \int_{t^{n-1}}^{t^{n+1}} \|\mathbf{u}_{ttt}\|^2 dt + \frac{\nu}{28} \|\nabla F[\phi_h^{n+1}]\| \end{aligned} \quad (5.17)$$

$$\begin{aligned} \nu(\nabla(F[\mathbf{u}^{n+1}] - \mathbf{u}_{n+1}), \nabla F[\phi_h^{n+1}]) &\leq C\nu \|\nabla(F[\mathbf{u}^{n+1}] - \mathbf{u}_{n+1})\|^2 + \frac{\nu}{28} \|\nabla F[\phi_h^{n+1}]\|^2 \\ &\leq C\nu \Delta t^3 \int_{t^{n-1}}^{t^{n+1}} \|\nabla \mathbf{u}_{tt}\|^2 dt + \frac{\nu}{28} \|\nabla F[\phi_h^{n+1}]\|^2. \end{aligned}$$

To bound the convective terms in $Intp(\mathbf{u}, F[\phi_h^{n+1}])$, we first rearrange the terms. Adding and subtracting terms for the convective terms and using the definition of the EMAC formulation, one gets

$$\begin{aligned}
& c(F[\mathbf{u}^{n+1}], F[\mathbf{u}^{n+1}], F[\phi_h^{n+1}]) - c(\mathbf{u}^{n+1}, \mathbf{u}^{n+1}, F[\phi_h^{n+1}]) \\
&= c(F[\mathbf{u}^{n+1}] - \mathbf{u}^{n+1}, F[\mathbf{u}^{n+1}], F[\phi_h^{n+1}]) + c(\mathbf{u}^{n+1}, F[\mathbf{u}^{n+1}] - \mathbf{u}^{n+1}, F[\phi_h^{n+1}]) \\
&= (F[\mathbf{u}^{n+1}] \cdot \nabla(F[\mathbf{u}^{n+1}] - \mathbf{u}^{n+1}), F[\phi_h^{n+1}]) + (F[\phi_h^{n+1}] \cdot \nabla F[\mathbf{u}^{n+1}] - \mathbf{u}^{n+1}), F[\mathbf{u}^{n+1}]) \\
&- ((F[\mathbf{u}^{n+1}] - \mathbf{u}^{n+1}) \cdot \nabla F[\mathbf{u}^{n+1}], F[\phi_h^{n+1}]) - ((F[\mathbf{u}^{n+1}] - \mathbf{u}^{n+1}) \cdot \nabla F[\phi_h^{n+1}], F[\mathbf{u}^{n+1}]) \\
&+ ((F[\mathbf{u}^{n+1}] - \mathbf{u}^{n+1}) \cdot \nabla \mathbf{u}^{n+1}, F[\phi_h^{n+1}]) + (F[\phi_h^{n+1}] \cdot \nabla \mathbf{u}^{n+1}, F[\mathbf{u}^{n+1}] - \mathbf{u}^{n+1})) \\
&- (\mathbf{u}^{n+1} \cdot \nabla(F[\mathbf{u}^{n+1}] - \mathbf{u}^{n+1}), F[\phi_h^{n+1}]) - (\mathbf{u}^{n+1} \cdot \nabla F[\phi_h^{n+1}], (F[\mathbf{u}^{n+1}] - \mathbf{u}^{n+1})) \tag{5.18}
\end{aligned}$$

Then, the convective terms in (5.18) are estimated by applying the Cauchy-Schwarz Inequality, and Young's inequalities together with the integral remainder form of Taylors theorem

$$\begin{aligned}
& |(F[\mathbf{u}^{n+1}] \cdot \nabla(F[\mathbf{u}^{n+1}] - \mathbf{u}^{n+1}), F[\phi_h^{n+1}])| \\
&\leq C\nu^{-1} \|\nabla F[\mathbf{u}^{n+1}]\|^2 \|\nabla(F[\mathbf{u}^{n+1}] - \mathbf{u}^{n+1})\|^2 + \frac{\nu}{28} \|\nabla F[\phi_h^{n+1}]\|^2 \\
&\leq C\nu^{-1} \Delta t^3 \|\nabla F[\mathbf{u}^{n+1}]\|^2 \int_{t_{n-1}}^{t_{n+1}} \|\nabla \mathbf{u}_{tt}\|^2 dt + \frac{\nu}{28} \|\nabla F[\phi_h^{n+1}]\|^2 \tag{5.19}
\end{aligned}$$

$$\begin{aligned}
& |(F[\phi_h^{n+1}] \cdot \nabla F[\mathbf{u}^{n+1}] - \mathbf{u}^{n+1}), F[\mathbf{u}^{n+1}])| \\
&\leq C\nu^{-1} \|\nabla F[\mathbf{u}^{n+1}]\|^2 \|\nabla(F[\mathbf{u}^{n+1}] - \mathbf{u}^{n+1})\|^2 + \frac{\nu}{28} \|\nabla F[\phi_h^{n+1}]\|^2 \\
&\leq C\nu^{-1} \Delta t^3 \|\nabla F[\mathbf{u}^{n+1}]\|^2 \int_{t_{n-1}}^{t_{n+1}} \|\nabla \mathbf{u}_{tt}\|^2 dt + \frac{\nu}{28} \|\nabla F[\phi_h^{n+1}]\|^2 \tag{5.20}
\end{aligned}$$

$$\begin{aligned}
& |-((F[\mathbf{u}^{n+1}] - \mathbf{u}^{n+1}) \cdot \nabla F[\mathbf{u}^{n+1}], F[\phi_h^{n+1}])| \\
&\leq C\nu^{-1} \|\nabla F[\mathbf{u}^{n+1}]\|^2 \|\nabla(F[\mathbf{u}^{n+1}] - \mathbf{u}^{n+1})\|^2 + \frac{\nu}{28} \|\nabla F[\phi_h^{n+1}]\|^2 \\
&\leq C\nu^{-1} \Delta t^3 \|\nabla F[\mathbf{u}^{n+1}]\|^2 \int_{t_{n-1}}^{t_{n+1}} \|\nabla \mathbf{u}_{tt}\|^2 dt + \frac{\nu}{28} \|\nabla F[\phi_h^{n+1}]\|^2 \tag{5.21}
\end{aligned}$$

$$\begin{aligned}
& |-((F[\mathbf{u}^{n+1}] - \mathbf{u}^{n+1}) \cdot \nabla F[\phi_h^{n+1}], F[\mathbf{u}^{n+1}])| \\
&\leq C\nu^{-1} \|\nabla F[\mathbf{u}^{n+1}]\|^2 \|\nabla(F[\mathbf{u}^{n+1}] - \mathbf{u}^{n+1})\|^2 + \frac{\nu}{28} \|\nabla F[\phi_h^{n+1}]\|^2 \\
&\leq C\nu^{-1} \Delta t^3 \|\nabla F[\mathbf{u}^{n+1}]\|^2 \int_{t_{n-1}}^{t_{n+1}} \|\nabla \mathbf{u}_{tt}\|^2 dt + \frac{\nu}{28} \|\nabla F[\phi_h^{n+1}]\|^2 \tag{5.22}
\end{aligned}$$

$$\begin{aligned}
& |((F[\mathbf{u}^{n+1}] - \mathbf{u}^{n+1}) \cdot \nabla \mathbf{u}^{n+1}, F[\phi_h^{n+1}])| \\
&\leq C\nu^{-1} \|\nabla \mathbf{u}^{n+1}\|^2 \|\nabla(F[\mathbf{u}^{n+1}] - \mathbf{u}^{n+1})\|^2 + \frac{\nu}{28} \|\nabla F[\phi_h^{n+1}]\|^2 \\
&\leq C\nu^{-1} \Delta t^3 \|\nabla \mathbf{u}^{n+1}\|^2 \int_{t_{n-1}}^{t_{n+1}} \|\nabla \mathbf{u}_{tt}\|^2 dt + \frac{\nu}{28} \|\nabla F[\phi_h^{n+1}]\|^2 \tag{5.23}
\end{aligned}$$

$$\begin{aligned}
& |(F[\phi_h^{n+1}] \cdot \nabla \mathbf{u}^{n+1}, F[\mathbf{u}^{n+1}] - \mathbf{u}^{n+1}))| \\
&\leq C\nu^{-1} \|\nabla \mathbf{u}^{n+1}\|^2 \|\nabla(F[\mathbf{u}^{n+1}] - \mathbf{u}^{n+1})\|^2 + \frac{\nu}{28} \|\nabla F[\phi_h^{n+1}]\|^2 \\
&\leq C\nu^{-1} \Delta t^3 \|\nabla \mathbf{u}^{n+1}\|^2 \int_{t_{n-1}}^{t_{n+1}} \|\nabla \mathbf{u}_{tt}\|^2 dt + \frac{\nu}{28} \|\nabla F[\phi_h^{n+1}]\|^2 \tag{5.24}
\end{aligned}$$

$$\begin{aligned}
& |-(\mathbf{u}^{n+1} \cdot \nabla(F[\mathbf{u}^{n+1}] - \mathbf{u}^{n+1}), F[\phi_h^{n+1}]))| \\
& \leq C\nu^{-1} \|\nabla \mathbf{u}^{n+1}\|^2 \|\nabla(F[\mathbf{u}^{n+1}] - \mathbf{u}^{n+1})\|^2 + \frac{\nu}{28} \|\nabla F[\phi_h^{n+1}]\|^2 \\
& \leq C\nu^{-1} \Delta t^3 \|\nabla \mathbf{u}^{n+1}\|^2 \int_{t_{n-1}}^{t_{n+1}} \|\nabla \mathbf{u}_{tt}\|^2 dt + \frac{\nu}{28} \|\nabla F[\phi_h^{n+1}]\|^2
\end{aligned} \tag{5.25}$$

$$\begin{aligned}
& |-(\mathbf{u}^{n+1} \cdot \nabla F[\phi_h^{n+1}], (F[\mathbf{u}^{n+1}] - \mathbf{u}^{n+1}))| \\
& \leq C\nu^{-1} \|\nabla \mathbf{u}^{n+1}\|^2 \|\nabla(F[\mathbf{u}^{n+1}] - \mathbf{u}^{n+1})\|^2 + \frac{\nu}{28} \|\nabla F[\phi_h^{n+1}]\|^2 \\
& \leq C\nu^{-1} \Delta t^3 \|\nabla \mathbf{u}^{n+1}\|^2 \int_{t_{n-1}}^{t_{n+1}} \|\nabla \mathbf{u}_{tt}\|^2 dt + \frac{\nu}{28} \|\nabla F[\phi_h^{n+1}]\|^2
\end{aligned} \tag{5.26}$$

Inserting (5.19)-(5.26) into (5.8) gives

$$\begin{aligned}
& \frac{1}{\Delta t} \left\| \begin{bmatrix} \phi_h^{n+1} \\ \phi_h^n \end{bmatrix} \right\|_G^2 - \frac{1}{\Delta t} \left\| \begin{bmatrix} \phi_h^n \\ \phi_h^{n-1} \end{bmatrix} \right\|_G^2 + \frac{1}{4\Delta t} \|\phi_h^{n+1} - 2\phi_h^n + \phi_h^{n-1}\|_F^2 + \frac{\nu}{2} \|\nabla F[\phi_h^{n+1}]\|^2 \\
& \leq \frac{C\nu^{-1}}{\Delta t} \int_{t^{n-1}}^{t_{n+1}} \|\eta_t\|^2 dt + C\nu \|\nabla F[\eta^{n+1}]\|^2 + C\nu^{-1} \inf_{q_h \in Q_h} \|P^{n+1} - q_h\|^2 \\
& \quad + C\nu^{-1} \Delta t^3 \int_{t_{n-1}}^{t_{n+1}} \|\mathbf{u}_{ttt}\|^2 dt + C\nu \Delta t^3 \int_{t_{n-1}}^{t_{n+1}} \|\nabla \mathbf{u}_{tt}\|^2 dt \\
& \quad + C\nu^{-1} \Delta t^3 (\|\nabla F[\mathbf{u}^{n+1}]\|^2 + \|\nabla \mathbf{u}^{n+1}\|^2) \int_{t_{n-1}}^{t_{n+1}} \|\nabla \mathbf{u}_{tt}\|^2 dt \\
& \quad + C\nu^{-1} \left(\|\nabla F[\mathbf{u}^{n+1}]\|^2 \|F[\eta^{n+1}]\| \|\nabla F[\eta^{n+1}]\| + \|\nabla F[\mathbf{u}^{n+1}]\| \|F[\mathbf{u}^{n+1}]\| \|\nabla F[\eta^{n+1}]\|^2 \right) \\
& \quad + C\nu^{-1} \|\nabla F[\mathbf{u}^{n+1}]\|^2 \|F[\phi_h^{n+1}]\|^2
\end{aligned}$$

Multiplying by Δt , summing from $n = 1$ to $n = N - 1$ and using approximation properties (2.4)-(2.5) yields

$$\begin{aligned}
& \left\| \begin{bmatrix} \phi_h^N \\ \phi_h^{N-1} \end{bmatrix} \right\|_G^2 + \frac{1}{4} \|\phi_h^{n+1} - 2\phi_h^n + \phi_h^{n-1}\|_F^2 + \frac{\nu \Delta t}{2} \|\nabla F[\phi_h^{n+1}]\|^2 \\
& \leq \left\| \begin{bmatrix} \phi_h^1 \\ \phi_h^0 \end{bmatrix} \right\|_G^2 + C \left(\nu^{-1} h^{2k+2} \|\mathbf{u}_t\|_{2,k+1}^2 + \nu h^{2k} \|\mathbf{u}\|_{2,k+1}^2 + \nu^{-1} h^{2k} \|P^{n+1}\|_{2,k}^2 \right) \\
& \quad + C\nu^{-1} \Delta t^4 \|\mathbf{u}_{ttt}\|_{L^2(0,T;L^2(\Omega))}^2 + C\Delta t^4 (\nu + \nu^{-1} (\|\nabla F[\mathbf{u}^{n+1}]\|_{\infty,0} + \|\nabla \mathbf{u}^{n+1}\|_{\infty,0})) \|\nabla \mathbf{u}_{tt}\|_{L^2(0,T;L^2(\Omega))}^2 \\
& \quad + C\nu^{-1} \left(\|\nabla F[\mathbf{u}^{n+1}]\|_{\infty,0} h^{2k+1} \|\mathbf{u}\|_{2,k+1}^2 + \|\nabla F[\mathbf{u}^{n+1}]\|_{\infty,0} \|F[\mathbf{u}^{n+1}]\|_{\infty,0} h^{2k} \|\mathbf{u}\|_{2,k+1}^2 \right) \\
& \quad + C\nu^{-1} \|\nabla F[\mathbf{u}^{n+1}]\|_{\infty,0} \Delta t \sum_{n=1}^{N-1} \|F[\phi_h^{n+1}]\|^2
\end{aligned} \tag{5.27}$$

Applying the discrete Gronwall inequality with the assumption

$$\Delta t \leq C(\|\nabla F[\mathbf{u}^{n+1}]\|_{\infty,0})^{-1}$$

and using Lemma 3.3 produces

$$\begin{aligned}
& \left\| \phi_h^N \right\|^2 + \frac{1}{3} \sum_{n=1}^{N-1} \left\| \phi_h^{n+1} - 2\phi_h^n + \phi_h^{n-1} \right\|_F^2 + \frac{2\Delta t \nu}{3} \sum_{n=1}^{N-1} \left\| \nabla F[\phi_h^{n+1}] \right\|^2 \\
& \leq \left(\frac{1}{3} \right)^N \left\| \phi_h^0 \right\|^2 + 2N(\left\| \phi_h^1 \right\|^2 + \left\| \phi_h^0 \right\|^2) + C \left[\nu^{-1} h^{2k+2} \left\| \mathbf{u}_t \right\|_{2,k+1}^2 + \nu h^{2k} \left\| \mathbf{u} \right\|_{2,k+1}^2 + \nu^{-1} h^{2k} \left\| P^{n+1} \right\|_{2,k}^2 \right. \\
& \quad \left. + \nu^{-1} \Delta t^4 \left\| \mathbf{u}_{ttt} \right\|_{L^2(0,T;L^2(\Omega))}^2 + \Delta t^4 (\nu + \nu^{-1} (\left\| \nabla F[\mathbf{u}^{n+1}] \right\|_{\infty,0} + \left\| \nabla \mathbf{u}^{n+1} \right\|_{\infty,0})) \left\| \nabla \mathbf{u}_{tt} \right\|_{L^2(0,T;L^2(\Omega))}^2 \right. \\
& \quad \left. + \nu^{-1} \left(\left\| \nabla F[\mathbf{u}^{n+1}] \right\|_{\infty,0} h^{2k+1} \left\| \mathbf{u} \right\|_{2,k+1}^2 + \left\| \nabla F[\mathbf{u}^{n+1}] \right\|_{\infty,0} \left\| F[\mathbf{u}^{n+1}] \right\|_{\infty,0} h^{2k} \left\| \mathbf{u} \right\|_{2,k+1}^2 \right) \right] \quad (5.28)
\end{aligned}$$

The final result follows from the triangle inequality. \square

6 Numerical Experiments

In this section, we perform four different numerical experiments to test the effectiveness of the proposed algorithm (3.3)-(3.5) and compare the results with the non-filtered BE-EMAC scheme (step 1 without step 2). The first test confirms the order of convergence rates predicted in Corollary 5.1 for an analytic test problem with known solution. In second example, we check the energy, momentum and angular momentum conservation of the EMAC-FILTERED scheme in a Gresho problem. In third and fourth tests, we studied typical benchmark problems of flow around a cylinder and flow past a flat plate respectively, to demonstrate the superiority of EMAC-FILTERED method over BE-EMAC scheme. All simulations are carried out with the Taylor-Hood finite element pairs $(\mathbf{X}_h, Q_h) = (P_2, P_1)$ for velocity and pressure on triangular grids. The computations are performed with the public license finite element software package Freefem++ [30].

6.1 Convergence Rates

In this part, we verify the expected convergence rates of our numerical scheme (3.3)-(3.5) described by Corollary 5.1. For this purpose, we pick the analytical solution:

$$\mathbf{u} = \begin{pmatrix} \cos(y)e^t \\ \sin(x)e^t \end{pmatrix}, \quad p = (x - y)(1 + t)$$

with the kinematic viscosity $\nu = 1$ and from which the external force is determined so that (1.1) is satisfied. Computations are performed in the unit square domain $\Omega = [0, 1]^2$. The boundary conditions are enforced to be the true solution. The approximate solutions are computed on successive mesh refinements and the velocity errors are measured in the discrete norm $L^2(0, T; H^1(\Omega))$

$$\left\| \mathbf{u} - \mathbf{u}^h \right\|_{2,1} = \left\{ \Delta t \sum_{n=1}^N \left\| \mathbf{u}(t^n) - \mathbf{u}_n^h \right\|^2 \right\}^{1/2}.$$

To test the spatial convergence, we fixed the time step as $\Delta t = 0.00001$ with an end time $t = 10^{-4}$ to isolate the spatial error and calculate the errors for varying h . Results for errors and rates are shown in Table 1. In a similar manner, we fix the mesh size to $h = 1/128$ to compute temporal errors and convergence rates by using different time steps with an end time of $t = 1$, see Table 2. One can observe second order accuracy both in time and space, which is the optimal convergence rate found in Corollary 5.1.

h	$\ u - u^h\ _{2,1}$	Rate
1/4	2.32618e-6	—
1/8	5.80867e-7	2.00209
1/16	1.44272e-7	2.00938
1/32	3.5518e-8	2.0221
1/64	9.56472e-9	1.89275

Table 1: Spatial errors and rates

Δt	$\ u - u^h\ _{2,1}$	Rate
1/4	0.0281784	—
1/8	0.00693954	2.02165
1/16	0.00124549	2.47811
1/32	0.000227284	2.45412
1/64	4.08335e-5	2.4767

Table 2: Temporal errors and rates

6.2 Gresho Problem

The second experiment we consider is Gresho problem, which is also referred to as the 'standing vortex problem' [36, 37, 38]. The simulation starts with an initial condition \mathbf{u}_0 that is an exact solution of the steady Euler equations. On the domain $\Omega = (-0.5, 0.5)^2$ with $r = \sqrt{x^2 + y^2}$, the velocity and pressure solutions are defined by

$$\begin{aligned} r \leq 0.2 &: \begin{cases} \mathbf{u} = \begin{pmatrix} -5y \\ 5x \end{pmatrix}, p = 12.5r^2 + C_1 \end{cases} \\ 0.2 \leq r \leq 0.4 &: \begin{cases} \mathbf{u} = \begin{pmatrix} \frac{2y}{r} + 5y \\ \frac{2x}{r} - 5x \end{pmatrix}, p = 12.5r^2 - 20r + 4\log(r) + C_2 \end{cases} \\ r > 0.4 &: \begin{cases} \mathbf{u} = \begin{pmatrix} 0 \\ 0 \end{pmatrix}, p = 0 \end{cases} \end{aligned} \quad (6.1)$$

where

$$C_2 = (-12.5)(0.4)^2 + 20(0.4)^2 - 4\log(0.4), \quad C_1 = C_2 - 20(0.2) + 4\log(0.2).$$

The speed plot of this initial condition can be seen in Figure 1.

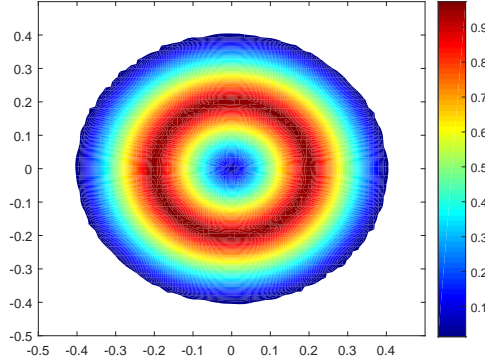


Figure 1: Speed contours of true solution of the Gresho problem at all times.

We compute solutions of the EMAC-FILTERED and BE-EMAC schemes by using Newton iterations to solve the nonlinear term with $\mathbf{f} = 0, \nu = 0$ and no penetration boundary conditions up to $T = 8$. The computations are run on a 48×48 uniform mesh with a time step size $\Delta t = 0.025$. Since the initial condition is the solution of the steady Euler equation, the accuracy of a method depends on keeping this solution over time. In addition, there is no any viscosity and forcing term, the problem is highly suitable to test the conservation properties of a numerical method. Plots of energy, momentum, angular momentum and L^2

error versus time of both the EMAC-FILTERED and BE-EMAC are shown in Figure 2. We note that L^2 errors of both schemes are computed by adding grad-div stabilization term. We see from the figure that both the EMAC-FILTERED and BE-EMAC schemes have the same accuracy and conserves energy, momentum and angular momentum, as expected while the EMAC-FILTERED scheme conserves energy better as time progresses which is clearly seen approximately after $t = 5$.

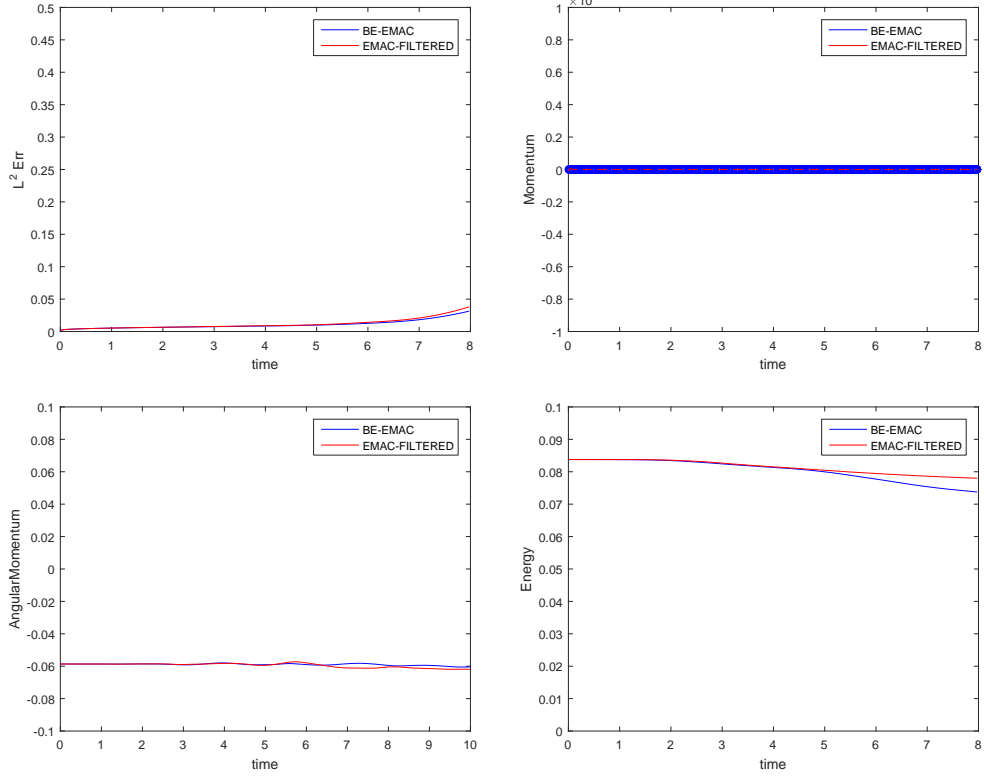


Figure 2: Plots of time versus L^2 error, energy, momentum and angular momentum.

6.3 Flow Around a Cylinder

In the next experiment, we test the performance of the EMAC-FILTERED algorithm on a famous benchmark problem taken from [41, 44], named channel flow around a cylinder and compare results with that of BE-EMAC scheme. This problem has been widely studied for simulation of fluid flows thanks to its real flow characteristics and highly reliable data to measure accuracy of methods. For the problem set-up, we follow the paper [44]. The computational domain is a $[0, 2.2] \times [0, 0.41]$ rectangular channel with a cylinder (circle) of radius 0.05 centred at $(0.2, 0.2)$, seen in Figure 3. The time dependent inflow and outflow velocity profiles are given by

$$\begin{aligned} \mathbf{u}_1(0, y, t) &= \mathbf{u}_1(2.2, y, t) = \frac{6}{0.41^2} \sin\left(\frac{\pi t}{8}\right) y(0.41 - y) \\ \mathbf{u}_2(0, y, t) &= \mathbf{u}_2(2.2, y, t) = 0 \end{aligned}$$

No-slip boundary conditions are enforced at the cylinder and walls. We take zero initial condition $\mathbf{u}(x, y, t) = 0$ and the kinematic viscosity $\nu = 10^{-3}$. Moreover, there is no external force acting on the flow. We run the

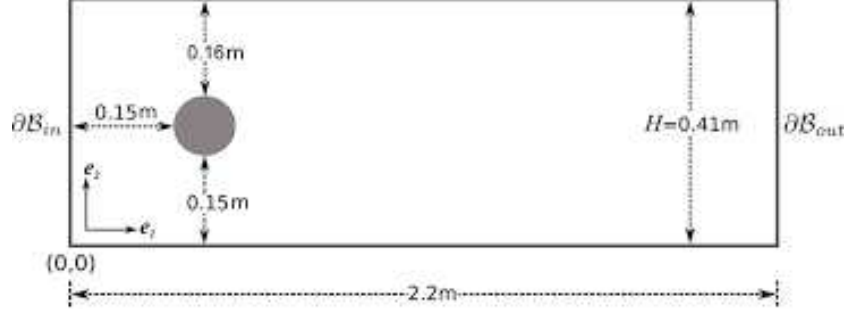


Figure 3: Domain Ω of the test problem

problem on a very coarse mesh consisting only 10210 total degrees of freedom with a last time $T = 8$ and time-step $\Delta t = 0.01$.

The plots of flow development of both BE-EMAC scheme and EMAC-FILTERED scheme at time $t = 2, 4, 6, 8$ are presented in Figure 4 and Figure 5, respectively. We observe that although BE-EMAC solutions at $t = 2, t = 4$ are similar to the DNS of [41, 44], solutions at $t = 6, t = 8$ are totally wrong in which even vortices are not formed which incorrectly predicts velocity solution of turbulent-like flows. However, the plots of EMAC-FILTERED scheme matches quite well with the DNS of [41, 44] in which the formation of vortices are clearly seen. This proves that EMAC-FILTERED scheme significantly improves the results of EMAC scheme.

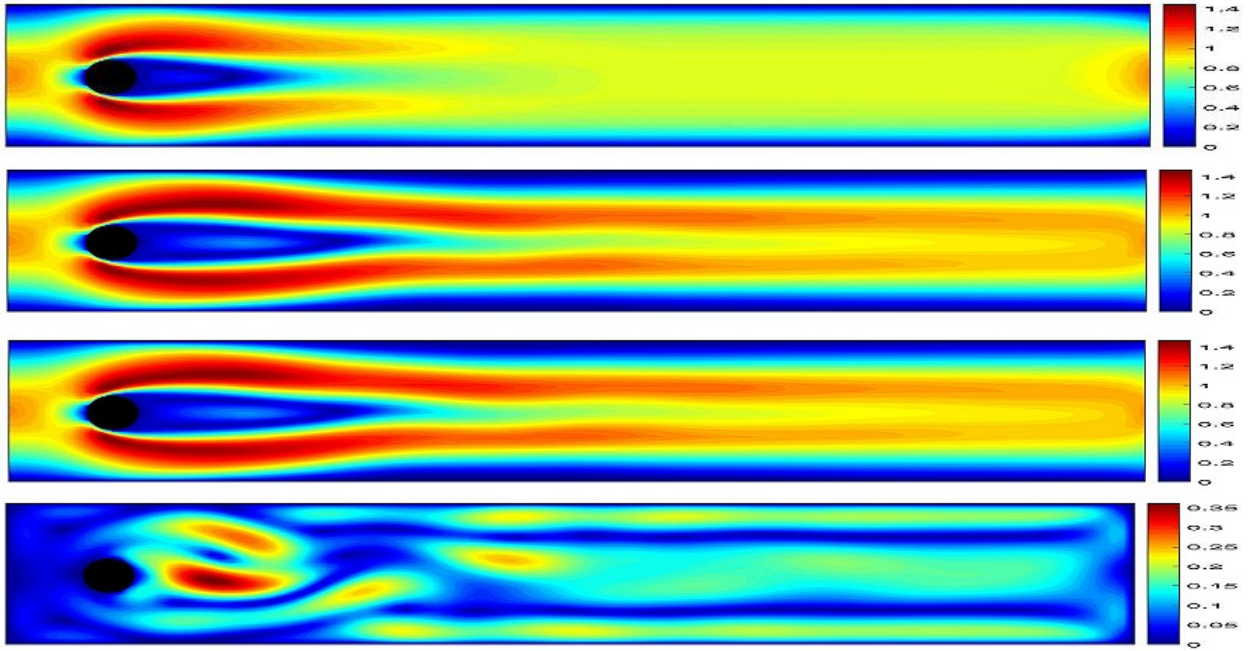


Figure 4: The velocity of the BE-EMAC scheme at $t = 2, 4, 6, 8$ (from up to down).

For further observation of the accuracy of our method (3.3)-(3.5), we look at the drag $c_d(t)$ and lift $c_l(t)$

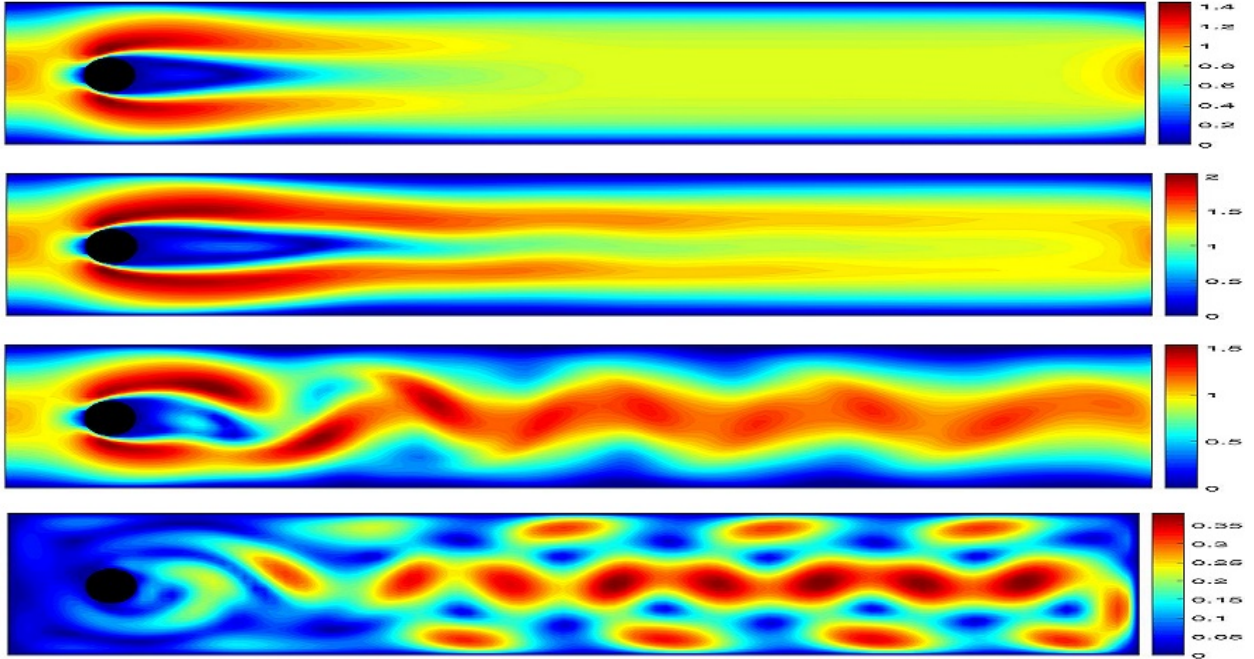


Figure 5: The velocity of the EMAC-FILTERED scheme at $t = 2, 4, 6, 8$ (from up to down).

coefficients at the cylinder. These values are defined in [44] as follows:

$$\begin{aligned} c_d(t) &= \frac{2}{\rho L U_{max}^2} \int_S (\rho \nu \frac{\partial \mathbf{u}_{ts}}{\partial n} n_y - p(t) n_x) dS \\ c_l(t) &= -\frac{2}{\rho L U_{max}^2} \int_S (\rho \nu \frac{\partial \mathbf{u}_{ts}}{\partial n} n_x + p(t) n_y) dS \end{aligned}$$

where S is the boundary of the cylinder, U_{max} is the maximum mean flow, L is the diameter of the cylinder, $n = (n_x, n_y)^T$ is the normal vector on the circular boundary S and \mathbf{u}_{ts} is the tangential velocity for $t_s = (n_y, -n_x)^T$ the tangential vector.

Table 3 shows the maximum drag ($c_{d,max}$) and maximum lift ($c_{l,max}$) values of both EMAC-FILTERED and BE-EMAC schemes behind the cylinder together with the times at which they occur. The following reference intervals are given in [41, 44]:

$$c_{d,max}^{ref} \in [2.93, 2.97], \quad c_{l,max}^{ref} \in [0.47, 0.49].$$

Comparing with the reference values, we see that while both predicts maximum drag coefficients correctly, EMAC-FILTERED scheme provides the best prediction of maximum lift coefficient compared with BE-EMAC scheme which is not even in the reference interval. This shows the superiority of EMAC-FILTERED scheme over EMAC scheme.

Method	$c_{d,max}$	$t(c_{d,max})$	$c_{l,max}$	$t(c_{l,max})$
EMAC-FILTERED	2.95281	3.94	0.468963	5.79
BE-EMAC	2.95215	3.93	0.0299554	7.13
Ref [41]	2.95092	3.93	0.47795	5.69

Table 3: Comparison of maximum drag and lift coefficients and the times at which they occur.

7 Flow Over a Flat Plate

In the last experiment, we continue to test the efficiency of the EMAC-FILTERED algorithm on a channel flow over a flat plate with $Re = 100$, taken from [39, 40]. It is modeled on a $[-7, 20] \times [-10, 10]$ rectangular channel with a 0.125×1 flat plate placed 7 units into the channel, and vertically centered. The problem setup is shown in Figure 6. We take inflow velocity as $\mathbf{u}_{in} = \langle 1, 0 \rangle$, zero-traction outflow and external force

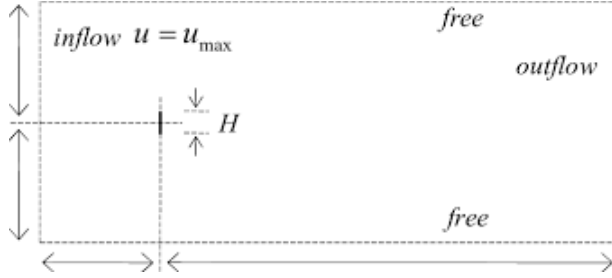


Figure 6: Domain Ω of the test problem

$\mathbf{f} = 0$. No-slip conditions are considered on the walls and plate. The simulation is run on a very coarse mesh consisting only 8745 total degrees of freedom with time step size $\Delta t = 0.02$ till the end time $T = 400$ s. The quantities of interest are the average value of drag coefficient and Strouhal number which are defined as

$$c_d(t) = \frac{2}{\rho L U_{max}^2} \int_S (\rho \nu \frac{\partial \mathbf{u}_{t_S}}{\partial n} n_y - p(t) n_x) dS$$

$$St = \frac{fL}{U_{max}}$$

where S is the plate, $n = (n_x, n_y)^T$ is the outward normal vector, \mathbf{u}_{t_S} is the tangential velocity for $t_S = (n_y, -n_x)^T$ the tangential vector, the density ρ_1 , f is the frequency of vortex shedding, the maximum inlet velocity is $U_{max} = 1$ and $L = 1$ is the length of the plate. Average drag values are computed using period-in-time state solutions over the time period $100 < t < 400$. The results are listed in Table 4. We observe that the average value of EMAC-FILTERED solution greatly matches with that of reference [39, 40] compared with that of BE-EMAC solution which is too far from the reference.

Method	$c_{d,avg}$
EMAC-FILTERED	2.64172
BE-EMAC	2.35042
Ref [12] (Very fine discretization)	2.6454
Ref [39]	2.60
Ref [40]	2.43

Table 4: The average drag coefficients.

8 Conclusion

In this paper, we proposed and analyzed the backward Euler based modular time filter method for the EMAC formulation of NSE. We showed that numerical accuracy is increased from first order to second order without requiring any additional computatational effort. Unconditional stability and convergence results that show optimal rates are provided. Several numerical experiments verify the theoretical convergence rates and demonstrate reliability and efficiency of the proposed method. The numerical results reveal that the EMAC-FILTERED scheme performs more accurate results and better quality solutions over the unfiltered case. We also showed that the EMAC-FILTERED scheme conserves important physical quantities like energy, momentum and angular momentum as good, or better than the BE-FEM.

References

- [1] D. Antonio, D. Pietro and A. Ern , Mathematical aspects of discontinuous Galerkin methods, Mathematics and Applications, Springer, Heidelberg **69** (2012).
- [2] V. Girault and P. A. Raviart, Finite element methods for Navier-Stokes equations, Springer Series in Computational Mathematics, Springer-Verlag, Berlin **5** (1986).
- [3] J. S. Hesthaven and T. Warburton, Nodal discontinuous Galerkin methods: Algorithms, analysis and applications, Springer Science and Business Media (2007).
- [4] W. Layton, Introduction to the Numerical Analysis of Incompressible Viscous Flows, SIAM (2008).
- [5] R. Temam, Navier-Stokes equations, Theory and Numerical Analysis, Stud. Math. Appl. **2** (1984).
- [6] T. Hughes, L. Mazzei, and K. Jansen, Large eddy simulation and the variational multiscale method, Comput. Vis. Sci. **3** (2000), 47–59.
- [7] R. E. Kalman, A new approach to linear filtering and prediction prolems, J. Basic Eng. **82(1)** (1960),33-45.
- [8] J. G. Liu and A. Wang, Energy and helicity preserving schemes for hydro and magnetohydro-dynamics flows with symmetry, J. Comput. Phys. **200** (2004), 8–33.
- [9] M. A. Olshanskii and L. G. Rebholz, A note on helicity balance of the Galerkin method for the 3D Navier-Stokes equations, Comput. Methods Appl. Math. **199** (2010), 1032–1035.
- [10] A. Palha and M. Gerritsma, A mass, energy, enstrophy and vorticity conserving (meevc) mimetic spectral element discretization for the 2D incompressible Navier-Stokes equations, arXiv preprint arXiv:1604.00257 (2016).
- [11] L. G. Rebholz, An energy and Helicity conserving finite element scheme for the Navier-Stokes equations, SIAM J. Numer. Anal. **45(4)** (2007), 1622–1638.

- [12] S. Charnyi, T. Heister, M. Olshanskii and L. Reholz, On conservation laws of Navier-Stokes Galerkin discretizations, *J. Comput. Phys.* **337** (2017), 289–308.
- [13] S. Charnyi, T. Heister, M. Olshanskii and L. Reholz, Efficient discretizations for the emac formulation of the incompressible Navier-Stokes equations, *Appl. Numer. Math.* **141** (2019), 220–233.
- [14] O. Lehmkuhl, F. Sacco, B. Paun, T. Iles, P. Iaizzo, G. Houzeaux, M. Vzaquex, C. Butakoff and J. Aguadu-Sierra, Evaluating the roles of detailed endocardial structures on right ventricular haemodynamics by means of CFD simulations, *Int. J. Numer. Method Biomed. Eng.* **34** (2018), 1–14.
- [15] O. Lehmkuhl, F. Sacco, B. Paun, T. Iles, P. Iaizzo, G. Houzeaux, M. Vzaquex and C. Butakoff, J. Aguadu-Sierra, Left ventricular trabeculations decrease the wall shear stress and increase the intra-ventricular pressure drop in CFD simulations, *Frontiers in Physiology* **9** (2018), 1–15.
- [16] R. Martin, M. Soria, O. Lehmkul, A. Gorobets and A. Duen, Noise radiated by an open cavity at low Mach number: Effect of the cavity oscillation mode, *Int. J. Aeroacoust.* **18(6-7)** (2019), 647–668.
- [17] H. Owen, G. Chrysokentis, M. Avila, D. Mira, G. Houzeaux, R. Borrell, J. C. Cajas and O. Lehmkuhl, Wall-modeled large-eddy simulation in a finite element framework, *Int. J. Numer. Meth. Fluids* **92(1)** (2020), 20–37.
- [18] D. Pastrana, J. C. Cajas, O. Lehmkuhl, I. Rodrguez and G. Houzeaux, Large-eddy simulations of the vortex-induced vibration of a low mass ratio two-degree-of-freedom circular cylinder at subcritical Reynolds numbers, *Comput. Fluids* **173** (2018), 118–132.
- [19] O. Lehmkul, U. Piomelli and G. Houzeaux, On the extension of the integral lengthscale approximation model to complex geometries, *Int. J. Heat Fluid Fl.* **78(108422)** (2019), 1–12.
- [20] M. Olshanskii and L. Reholz, Longer time accuracy for incompressible Navier-Stokes simulations with the EMAC formulation, *Comput. Methods Appl. Mech. Engrg.* **372:113369** (2020), 1–12.
- [21] V. John, G. Matthies and J. A. Rang, Comparison of time-discretization/linearization approaches for the incompressible Navier-Stokes equation, *Comput. Methods Appl. Mech. Engrg.* **195** (2006), 5995–6010.
- [22] J. Frutos, B. Garcia-Archilla and J. Novo, The post-processed mixed finite-element method for the Navier-Stokes equations: refined error bounds, *SIAM J. Numer. Anal.* **46(1)** (2008), 201–230.
- [23] P. M. Gresho and R.L. Sani, Incompressible flow and the finite element method, Volume 2, Isothermal Laminar Flow, Wiley (1998).
- [24] A. Guzel and W. Layton, Time filters increase accuracy of the fully implicit method, *BIT* **58(2)** (2018), 301–315.
- [25] V. Decaria, W. Layton and H. Zhao, A time-accurate, adaptive discretization for fluid flow problems, *Int. J. Numer. Anal. Model.* **17(2)** (2020), 254–280.
- [26] A. Cibik, S. Kaya and F. G. Eroglu, Analysis of Second Order Time Filtered Backward Euler Method for MHD Equations, *J. Sci. Comput.* **82(2)** (2020), 696–713.
- [27] M. Akbas, An Adaptive Time Filter Based Finite Element Method for the Velocity-Vorticity-Temperature Model of the Incompressible Non-Isothermal Fluid Flows, *Gazi University Journal of Science* **33** (2020), 696–713.
- [28] V. John, Finite element methods for incompressible flow problems, Springer Ser. Comput. Math. Springer-Verlag, Berlin, **51** (2016).
- [29] S. C. Brenner and L. R. Scott, The mathematical theory of finite element methods, Texts in Applied Mathematics, Springer, Berlin **5** (2008).

- [30] F. Hecht, New development in Freefem++, *J. Numer. Math.* **20** (2012), 251–265.
- [31] J. Heywood and R. Rannacher, Finite element approximation of the nonstationary Navier-Stokes problem. part iv: Error analysis for the second order time discretization, *SIAM J. Numer. Anal.* **2** (1979).
- [32] V. Girault and P. A. Raviart, Finite element methods for the Navier-Stokes equations theory and algorithms, Springer-Verlag (1986)
- [33] D. N. Arnold, F. Brezzi and M. Fortin, A stable finite element for the Stokes equations, *Calcolo* **21(4)** (1984), 337–344.
- [34] E. Hairer and G. Wanner, Solving ordinary differential equations : stiff and differential algebraic problems, Springer-Verlag (2002).
- [35] N. Jiang, M. Mohebujjaman, L. G. Rebholz and C. Trenchea, An optimally accurate discrete regularization for second order time stepping methods for Navier-Stokes equations, *Comput. Methods Appl. Mech. Engrg.* **310** (2016), 388–405.
- [36] P. Gresho, On the theory of semi-implicit projection methods for viscous incompressible flow and its implementation via a finite element method that also introduces a nearly consistent mass matrix. Part 2: Applications, *Int. J. Numer. Meth. Fluids* **11** (1990), 621–659.
- [37] S. Ray, T. Tezduyar, S. Mittal and R. Shih, Incompressible flow computations with stabilized bilinear and linear equal-order-interpolation velocity-pressure elements, *Comput. Methods Appl. Mech. Engrg.* **95** (1992), 221–242.
- [38] R. Liska and B. Wendroff, Comparision of several difference schemes on 1D and 2D test problems for the Euler equations, *SIAM J. Sci. Comput.* **25** (2003), 995–1017.
- [39] A Saha, Far wake characteristics of two-dimensional flow past a normal flat plate, *Phys. Fluids* **19:128110** (2007), 1–4.
- [40] A Saha, Direct numerical simulation of two-dimensional flow past a normal flat plate, *J. Eng. Mechanics* **139(12)** (2013), 1894–1901.
- [41] _____, Reference values for drag and lift of a two-dimensional time-dependent flow around the cylinder, *Int. Numer. Meth. Fl.* **44** (2004), 777–788.
- [42] M. A. Olshanskii and L. G. Rebholz, A note on helicity balance of the Galerkin method for the 3D Navier-Stokes equations, *Comput. Methods Appl. Mech. Eng.* **199** (2010), 1032–1035.
- [43] L. G. Rebholz, Helicity and physical fidelity in turbulence modeling, Ph.D. thesis, University of Pittsburgh, 2006.
- [44] M. Shafer and S. Turek, Benchmark Computations of Laminar Flow Around Cylinder, E.H. Hirschel ed., *Flow Simulation with High-Performance Computers II*, Notes Numer. Fluid Mech., Vieweg, **52** (1996), 547–566.